LA-UR-19-24828
Approved for public release; distribution is unlimited.

Title: Annual IPCA2 Performance Report for JFY18

Author(s): Henzlova, Daniela Constance
Archuleta, Jeffrey Christopher
Andrews, Madison Theresa
Favalli, Andrea
Marlow, Johnna Boulds
Rael, Carlos D.
Swinhoe, Martyn Thomas

Intended for: Report

Issued: 2019-05-23

Annual IPCA2 Performance Report for JFY18

Prepared for:

Japan Atomic Energy Agency

Prepared by:

D. Henzlova[1], J. Archuleta[1], M.T. Andrews[2], A. Favalli[1], J.B. Marlow[1], C.D. Rael[1], M.T. Swinhoe[1]

[1] Safeguards Science and Technology Group (NEN-1)

[2] Monte Carlo Methods, Codes, and Applications Group (XCP-3)

Los Alamos National Laboratory

Los Alamos, NM 87545 USA

March 2019

This page is intentionally left blank.

Contents

Figures

Acronyms

cps	counts per second
FRAM	Fixed Energy Response Function Analysis with Multiple Efficiencies
HPGe	High Purity Germanium
IPCA2	Improved Plutonium Canister Assay System 2
LANL	Los Alamos National Laboratory
MOX	Mixed-OXide

1. Overview

This report summarizes the results of monthly control measurements of IPCA2 performed over the period of October 2018 through March 2019 and represents an annual performance overview for JFY18. Note that the start of the measurements in October 2018 was defined by the start of the contract agreement. Monthly measurements of Plutonium neutron detection efficiency, AmLi stability, Curium stability and HPGe gamma spectra of Plutonium standards were performed and analyzed. All the results are shown with respect to original control bounds established from 2013-2017 data in [1]. Updated control bounds established based on this JFY18 data for use during JFY19 measurements are summarized in Appendix A. Based on Pu efficiency measurements, the performance of the IPCA2 during this reporting period was stable within 0.6% at 1 σ level. Measurements were compared to room temperature and humidity and no dependence was found for any detector performance. The end of this report contains summary of all IPCA2 measurements performed since October 2018 and includes discussion of troubleshooting and repair activities performed over the reporting period.

2. Plutonium Efficiency

2.1. Efficiency Monitoring

Plutonium efficiency measurements were performed on monthly basis between October 2018 and March 2019. The LANL Plutonium standard, FZC157 (823.6 neutrons s^{-1} emission rate), was used in all measurements. This source was placed in the IPCA2 for a duration of 1800 s during which 60 cycles of 30 s were used to calculate a Singles rate (in counts per second, cps). The Singles rate was divided by source activity to determine an efficiency as shown in Figure 1. Average efficiency corresponding to the JFY18 control period was calculated and corresponds to 7.29 ± 0.04. All measurements were within the control chart 2σ bands, denoted with dotted lines in Figure 1, however, they appear systematically lower than average. We speculate that it could be due to the change in grounding of IPCA2 performed in October 2018 as its onset is correlated with this activity. The grounding was updated to mitigate sudden noise observed in the control measurements performed in early October, as discussed during JAEA visit (for further details see Section 8). Updated control bounds will be established based on the data shown in Figure 1 for use in JFY19 measurements. The updated control bounds are provided for reference in Appendix A. All the Pu efficiency measurements since May 2013 are summarized in Figure 2.

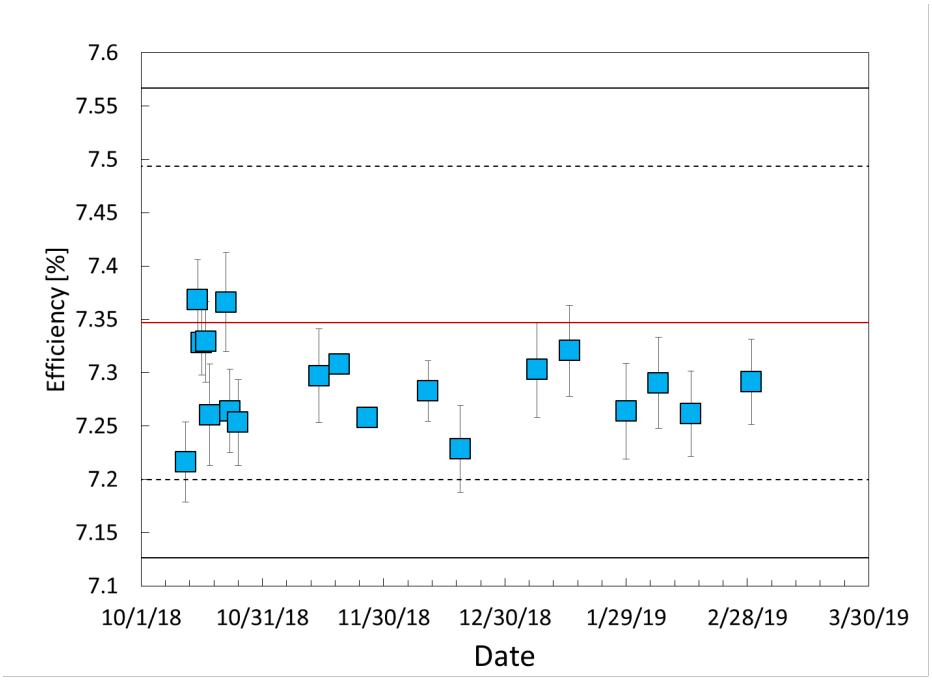

Figure 1: Pu efficiency measurements for JFY18.

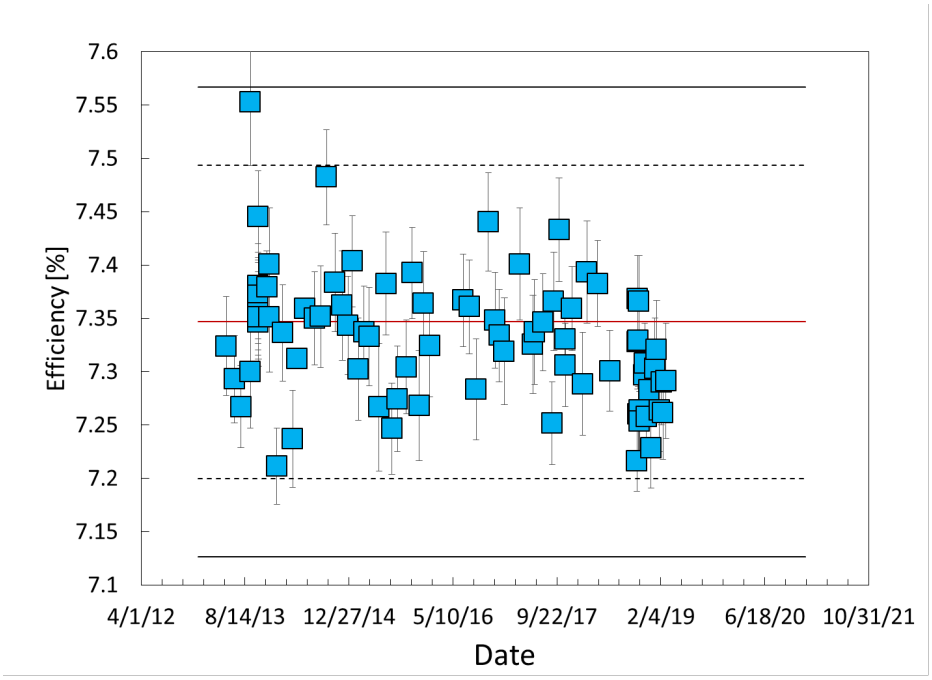

Figure 2: Pu efficiency measurements for May 2013 – March 2019.

2.1. Efficiency Dependence on Environmental Conditions

Room temperature and humidity data has been collected alongside IPCA2 measurements since October 2018. JFY18 plutonium efficiency measurements exhibit no dependence on humidity, Figure 3, or room temperature, Figure 4. Updated control bounds established from this JFY18 data and reported in Appendix A will be used for JFY19 control charts.

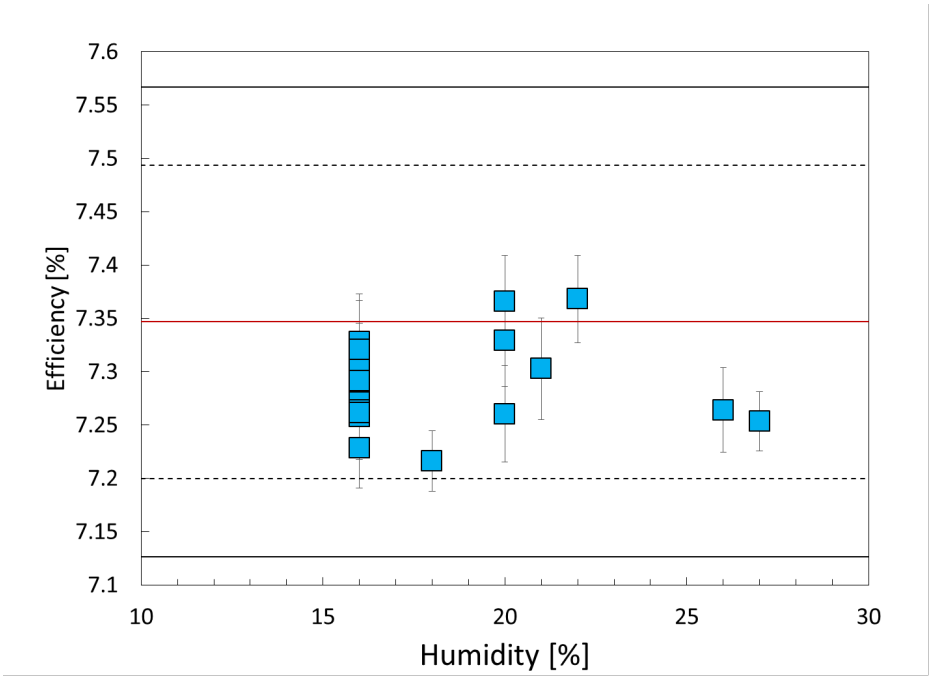

Figure 3: JFY18 Pu efficiency measurements as a function of humidity.

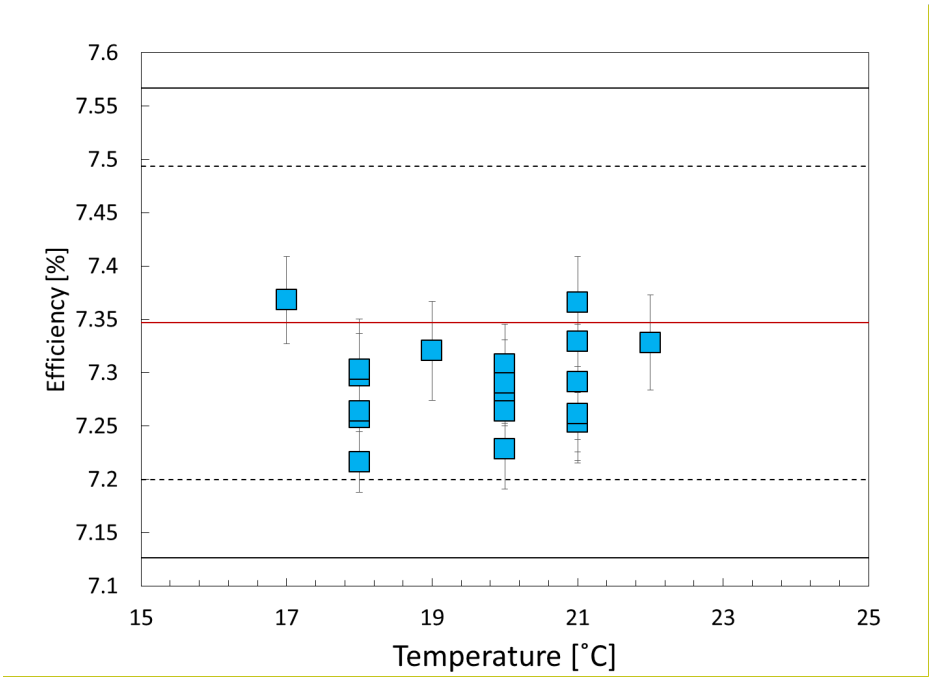

Figure 4: JFY18 Pu efficiency measurements as a function of room temperature.

3. AmLi Stability

3.1. AmLi Stability Measurements

AmLi stability measurements performed between October 2018 and March 2019 are summarized in Figure 5, with an average (decay corrected) count rate of 24484 ± 33. Overview of all decay corrected AmLi stability data from May 2013 is shown in Figure 6. Note that the decay correction on the AmLi data is with respect to 01/12/2017, when the current control bounds were established in [1]. Most results were within the 3σ control lines, however several anomalous results were observed in late 2016 and late 2018. As discussed in previous annual report [1], it is believed that source positioning and redistribution of contents of AmLi sources resulted in the observed variation of count rates. To mitigate this issue, we began to perform a Curium stability measurement in October 2018, to assess its feasibility as an alternative to AmLi; those measurements are described in the next section. No dependence of AmLi count rate on humidity or room temperature was observed, as shown in Figure 7 and Figure 8, respectively. Note that the data in Figure 5, 7 and 8 are systematically lower than average, which was established including the higher count rate data points shown in Figure 6 (see ref. [1]). New control bounds were established based on all JFY18 data for use in JFY19 control measurements and are reported in Appendix A.

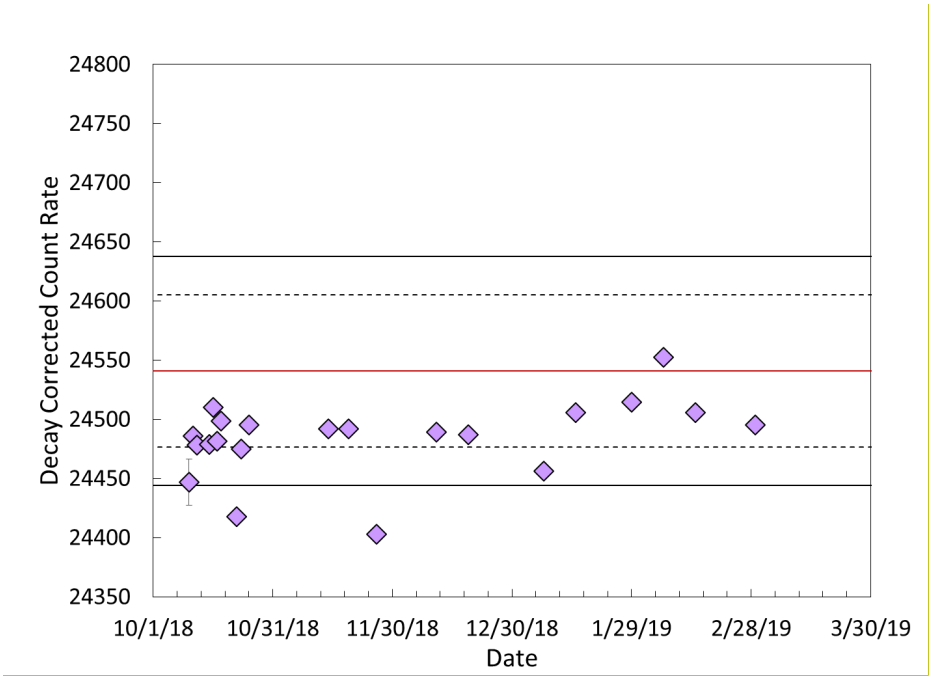

Figure 5: AmLi stability measurements for JFY18. Note that error bars are smaller than the size of symbols.

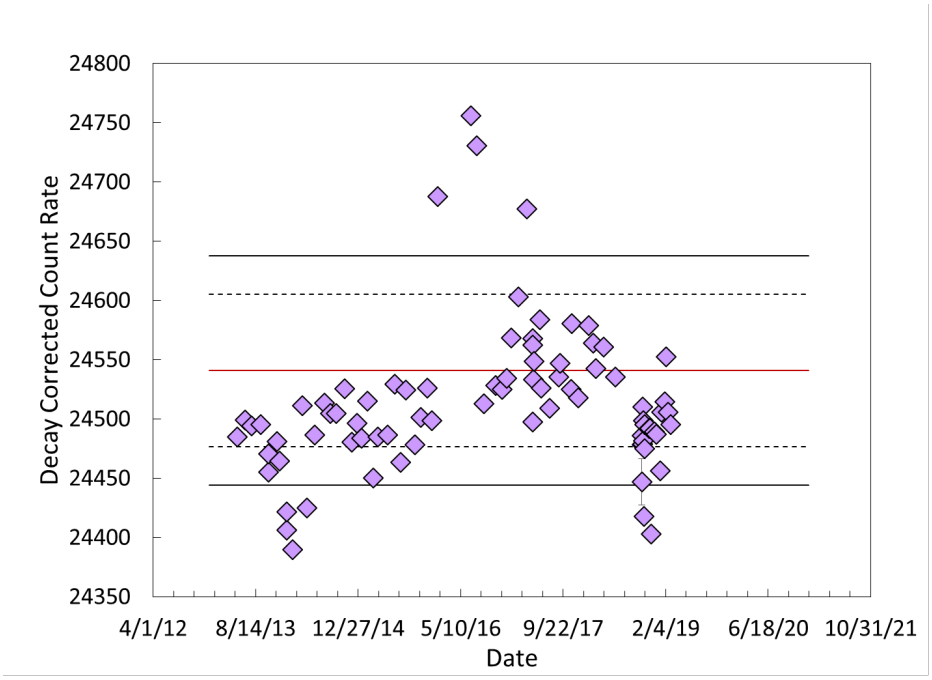

Figure 6: AmLi stability measurements from May 2013 – March 2019.

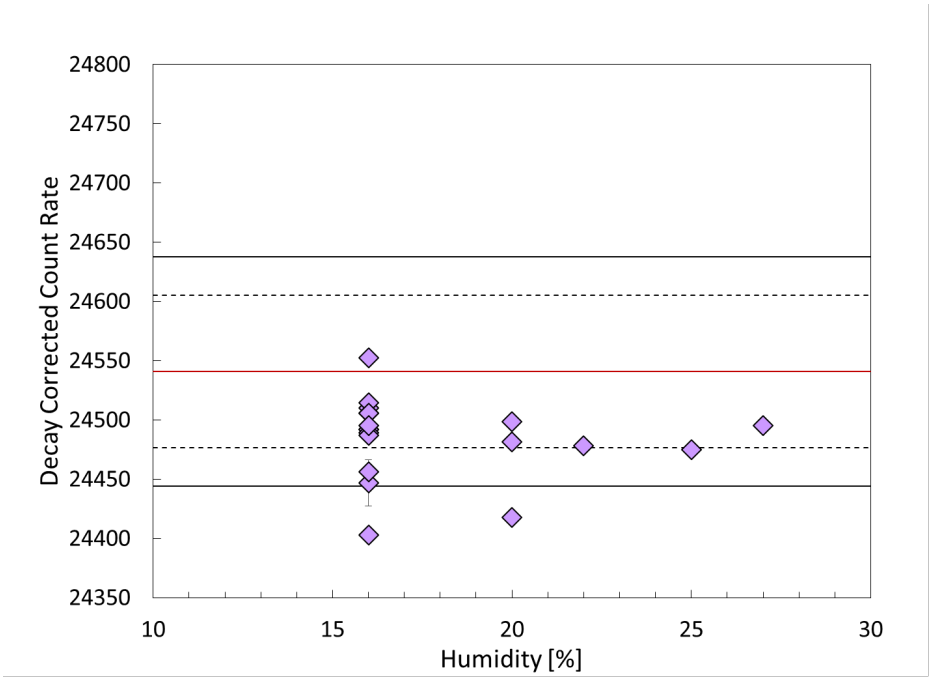

Figure 7: JFY18 AmLi stability measurements as a function of humidity.

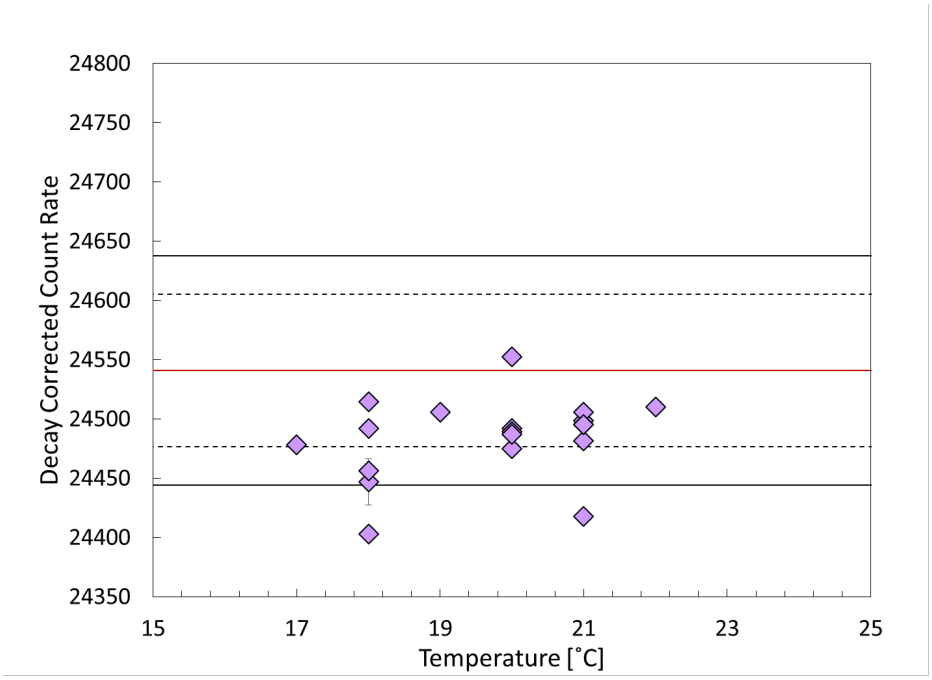

Figure 8: JFY18 AmLi stability measurements as a function of temperature.

4. Curium Stability

In October 2018 we started to perform monthly measurements with a Curium source to evaluate its feasibility as a potential replacement for the AmLi stability measurements. The decay corrected (with respect to the first measurement on 10/15/2018) results of all the Curium measurements performed over the reporting period are summarized in Figure 9 and correspond to an average count rate of 987.3 ± 2.0. Results reported here were used to establish new control bounds for Curium measurements shown in Figure 9 and Appendix A. Curium stability was also evaluated as a function of humidity and temperature as shown in Figure 10 and Figure 11, respectively. No dependence on humidity and room temperature has been observed over the reporting period.

Based on the trends observed so far, Curium appears to be a viable alternative to AmLi sources. Both sources will continue to be used during JFY19 control measurements.

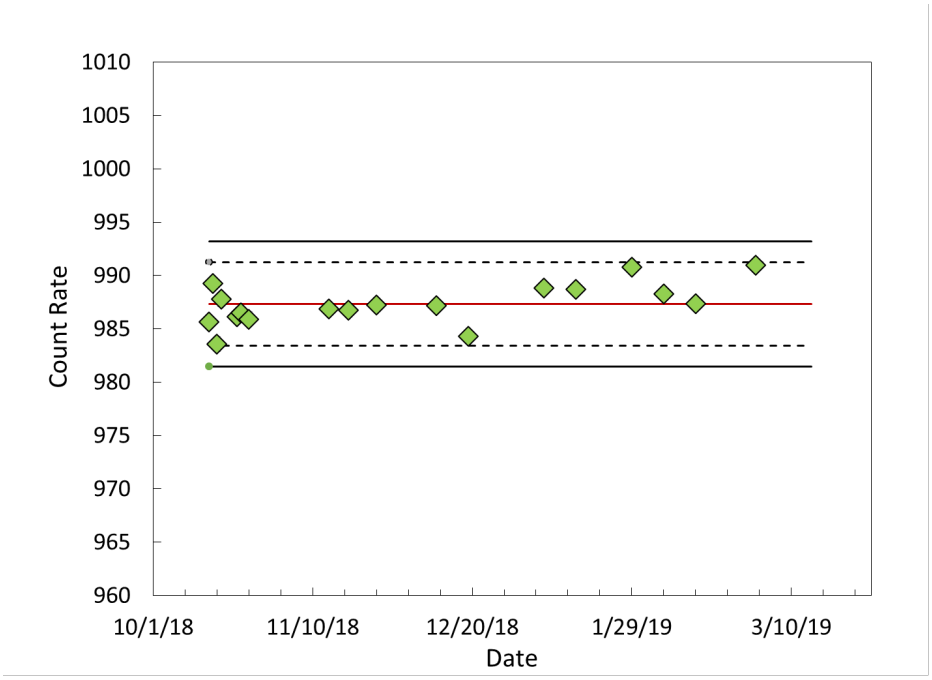

Figure 9: Curium count rates since for JFY18. Note that error bars are smaller than the size of symbols.

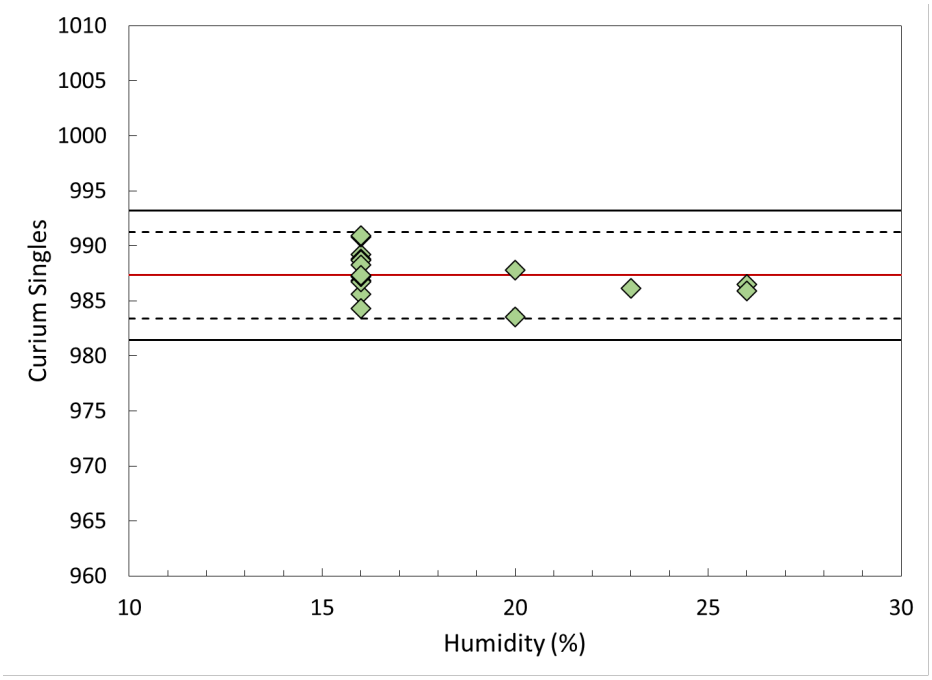

Figure 10: JFY18 Curium count rates as a function of humidity. Note that error bars are smaller than the size of symbols.

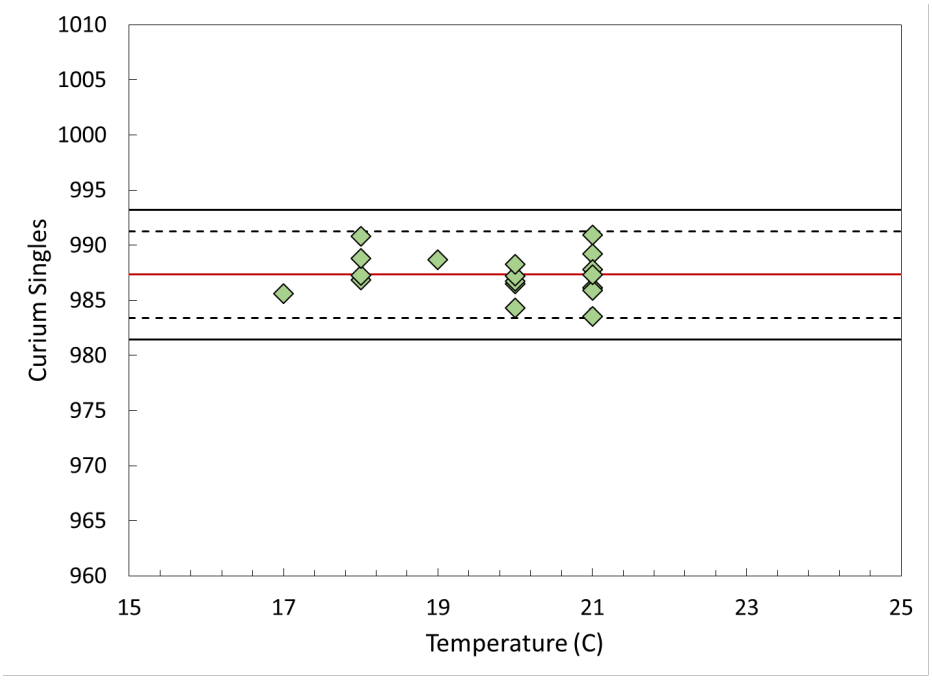

Figure 11: JFY18 Curium count rates as a function of room temperature. Note that error bars are smaller than the size of symbols.

5. HPGe System Performance

October 2018 through March 2019 period has seen many developments on HPGe system performance. Failure of middle (41993a) and bottom (4200a) HPGe detector systems was observed between December 2017 and February 2018. Initial troubleshooting was performed at the start of the new contract period in October 2018 and resulted in the resurrection of the middle (41993a) HPGe detector system by replacing the original X-Cooler and DSPEC with LANL spares. Further troubleshooting during January 2019 resulted in the resurrection of the bottom (4200A) HPGe detector system by replacement of the original X-Cooler with another LANL spare. Full summary of troubleshooting activities is provided in Section 8.1. Current component layout is described in the following section.

The October through December 2018 measurements therefore only included the two working HPGe detectors. The third (bottom) detector was included in the control charts again starting in January 2019.

An overview of all three HPGe detectors performance during October 2018 through March 2019 and over the full monitoring period (i.e. May 2013 – March 2019) is shown in Figures 13-18.

5.1. Current IPCA2 HPGe system configuration

The current configuration of HPGe system components as of February 2019 is shown in Figure 12. Two LANL X-Coolers are used on two of IPCA2 HPGe detectors. One LANL DSPEC is used on one of IPCA2 HPGe detectors.

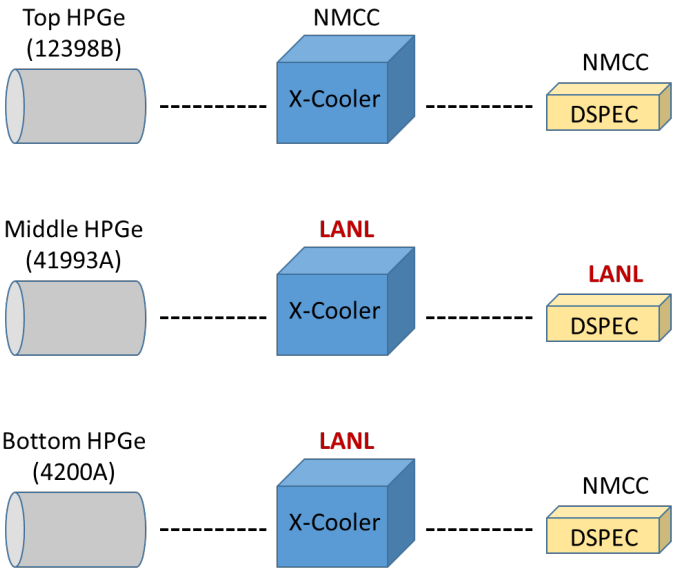

Figure 12: Configuration of IPCA2 HPGe system as of February 2019.

5.2. Top HPGe Detector Performance Summary

The top detector (12698B) shows a good performance over the entire measurement period for the $^{240}Pu/^{239}Pu$ ratio with the exception of December 19 measurement, which resulted in 0 ratio (Figure 13, left). The $^{241}Pu/^{239}Pu$ ratio for December 19 showed a very high value clearly outside the control bounds (Figure 14, left). This observation was discussed in more detail in the corresponding monthly report [4] and was attributed to a likely temporary failure of the detector cooling during that measurement period. As can be seen from all subsequent $^{240}Pu/^{239}Pu$ ratios, the performance was fully restored in the subsequent measurements. Several measurements in November 2018 through January 2019 resulted in $^{241}Pu/^{239}Pu$ ratios below the control bounds. The corresponding spectra exhibit slight broadening of peaks, which explains the low $^{241}Pu/^{239}Pu$ ratio and could most likely be explained by a temporary reduced cooling performance before and after the cooling failure observed on December 19. The data summarized in Figure 13, 14 (right), with the exception of December 19 data point and the low $^{241}Pu/^{239}Pu$ ratios will be used to establish updated control bounds for JFY19 control measurements.

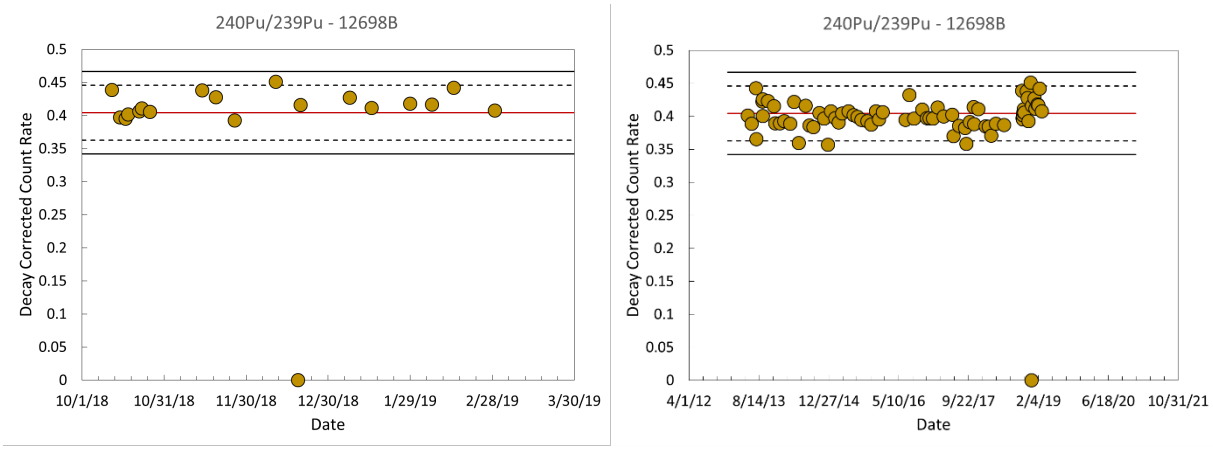

Figure 13: $^{240/239}$Pu isotopic ratios as determined by the top IPCA2 HPGe for JFY18 (left); for the entire measurement period (right).

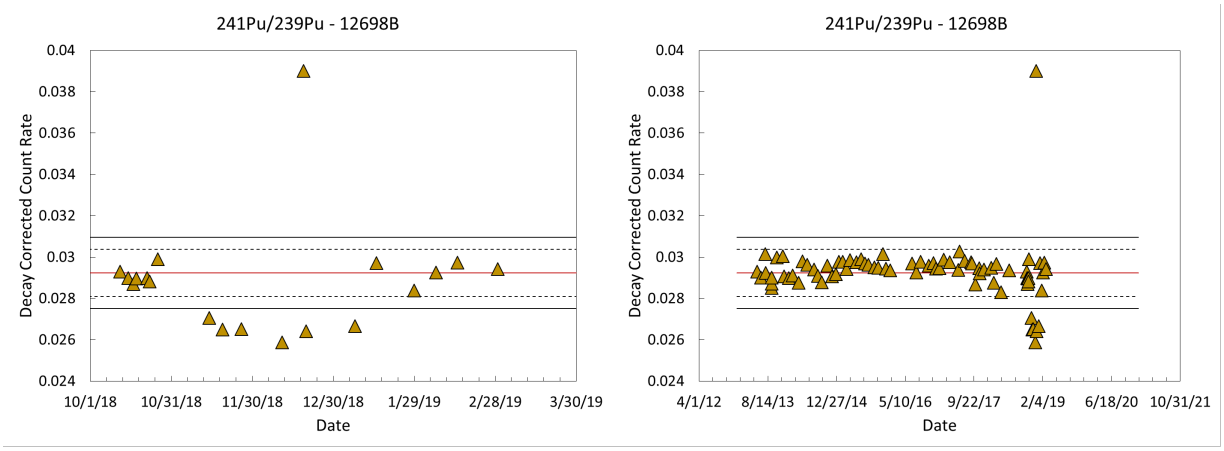

Figure 14: $^{241/239}$Pu isotopic ratios as determined by the top IPCA2 HPGe for JFY18 (left); for the entire measurement period (right).

5.3. Middle HPGe Detector Performance Summary

The middle HPGe detector shows a consistent performance over the entire evaluation period for both, ^{240}Pu/^{239}Pu and ^{241}Pu/^{239}Pu ratios. Note that a slight gain change was observed in December 11 and January 29 data as reported in [4,5], which was resolved by updating the standard gain value (0.125 keV/ch) to 0.1245 keV/ch. The data in Figures 15 and 16 show the corresponding ratio with the corrected gain for both dates.

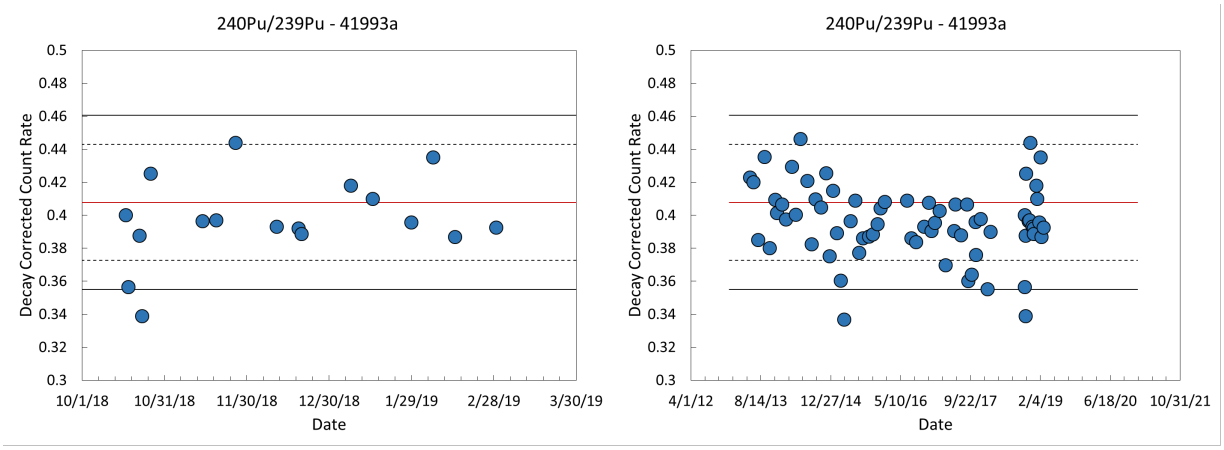

Figure 15: $^{240/239}$Pu isotopic ratios as determined by the middle IPCA2 HPGe for JFY18 (left); for the entire measurement period (right).

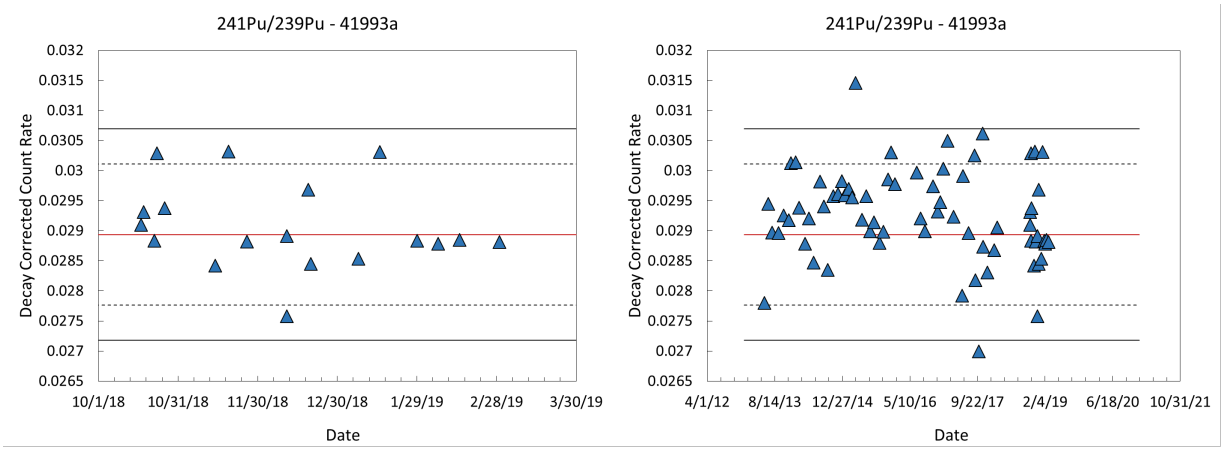

Figure 16: $^{241/239}$Pu isotopic ratios as determined by the middle IPCA2 HPGe for JFY18 (left); for the entire measurement period (right).

5.4. Bottom HPGe Detector Performance

As discussed earlier, the bottom HPGe detector system has not been operational until January 2019. The first measurement with the bottom detector was performed shortly after the X-Cooler replacement and exhibit ^{240}Pu/^{239}Pu and ^{241}Pu/^{239}Pu ratios just on the level of 3σ control lines as shown in Figures 17 and 18. The subsequent January measurements, however, reveal a good performance, suggesting that the cooling was likely incomplete when the first measurement was performed and therefore resulted in the less than optimal ratios.

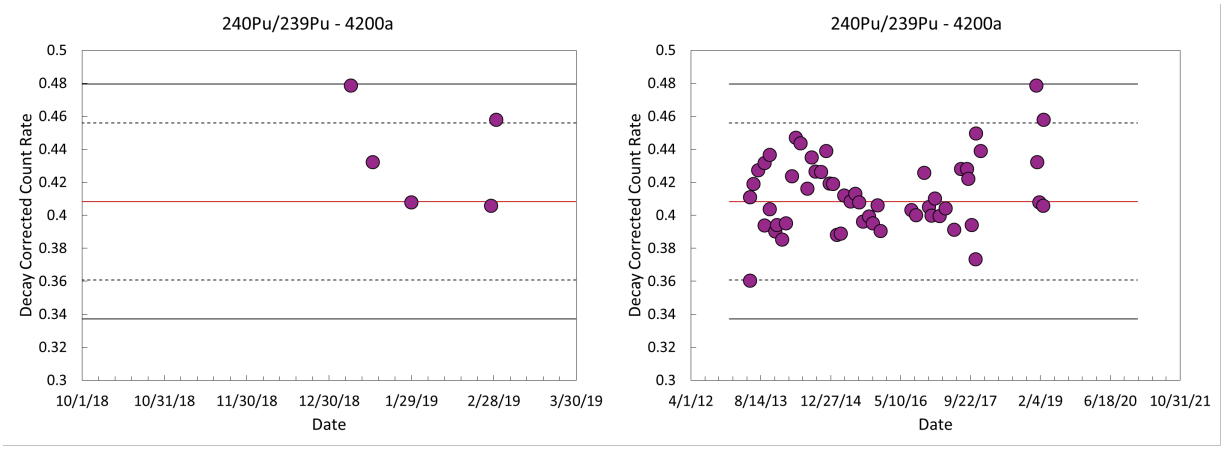

Figure 17: $^{240/239}$Pu isotopic ratios as determined by the bottom IPCA2 HPGe for JFY18 (left); for the entire measurement period (right).

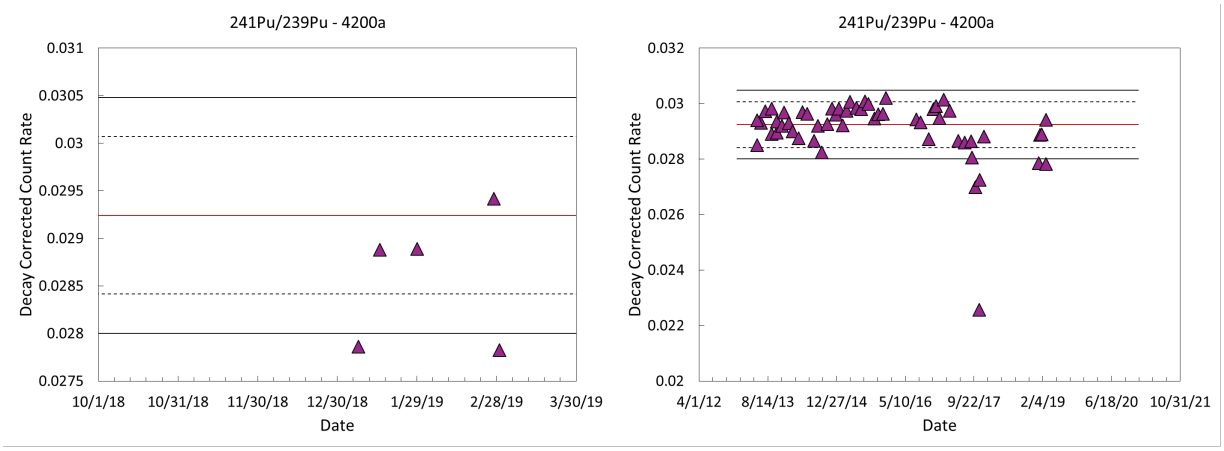

Figure 18: $^{241/239}$Pu isotopic ratios as determined by the bottom IPCA2 HPGe for JFY18 (left); for the entire measurement period (right).

6. Load Cell Data

Regular load cell measurements were performed during October 2018 - March 2019 period. Each of these measurements resulted in a consistent weight of 22.69 kg.

7. Continuous Background Monitoring

As part of the contractual agreement, continuous neutron system background was acquired for IPCA2 during November 2018 through March 2019. The measurements were performed using MIC software and analyzed with RadReview. Singles count rates over the reporting period are shown in Figure 19. The Singles background exhibits regular variation between approximately 25 – 32 counts per second, which can be attributed to variation in cosmic ray background. Figure 20 shows temperature and humidity recorded near IPCA2. The high count rate spikes and intervals seen in Singles background correspond to various measurements that are occasionally performed in the High Bay area, where IPCA2 is located. Note that the area is used as a test ground for other LANL developed instrumentation and experiments are routinely performed throughout the year.

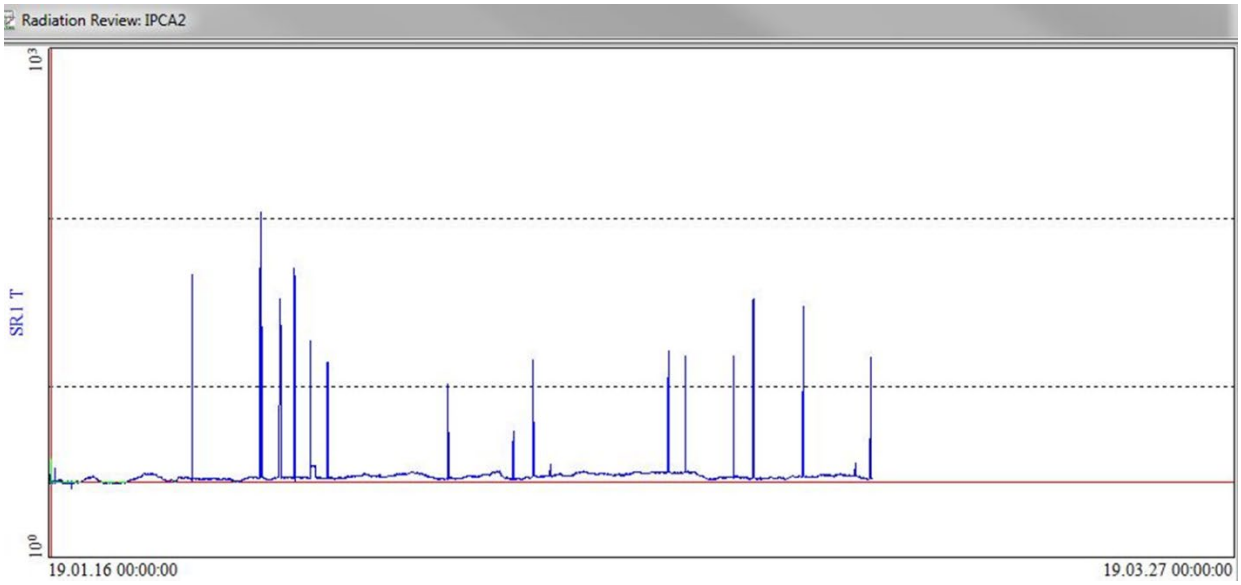

Figure 19: MIC recorded IPCA2 neutron background Singles over November 2018 through March 2019 period.

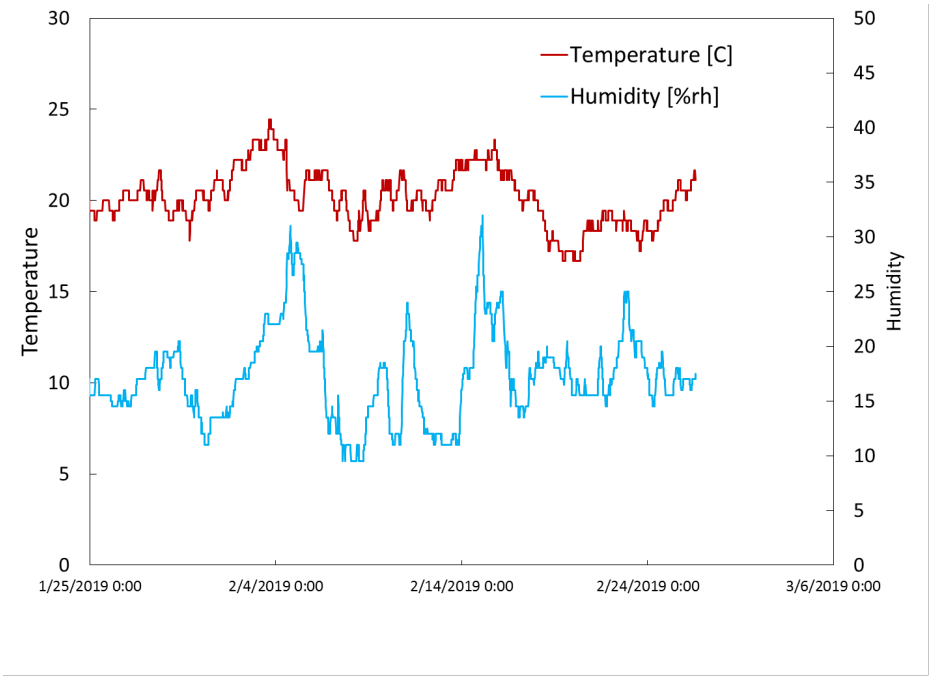

Figure 20: Environmental temperature and humidity recorded at IPCA2 location during the reporting period.

8. Troubleshooting and Repairs

This section provides an overview of all troubleshooting and repair activities performed between October 2018 and March 2019.

8.1. HPGe system troubleshooting and repairs

Failure of performance two of three IPCA2 HPGe detectors (middle (41993a) and bottom (4200a)) was observed between December 2017 and February 2018. Main troubleshooting activities were initiated with the start of new contract in October 2018. The troubleshooting involved evaluation of all the HPGe system components in order to establish if the HPGe detectors themselves are still operational. The activities focused on DSPECs and X-Coolers and involved soft resets (of DSPEC) and component replacements with LANL spares. Prior to these activities, pumping of the middle HPGe detector was also performed in summer 2018. The pumping had no effect on the observed performance failure.

Performed troubleshooting activities resulted in the resurrection of the middle (41993a) HPGe detector by replacing its X-Cooler and DSPEC with LANL spares. Both of these components appeared to have failed. The HPGe detector itself is fully operational as can be seen from results reported in Section 5.3.

Further troubleshooting of the bottom HPGe detector system was performed during January 2019, again focusing on DSPEC and X-Cooler components and resulted in replacement of the X-Cooler with another LANL spare unit. Following the X-Cooler replacement, the HPGe detector performed as expected as can be seen in Section 5.4.

8.1.1. Effect of HPGe detector pumping

During the October JAEA visit it was requested to provide a discussion of HPGe detector pumping on its performance. Note that the middle HPGe detector was not functional at the time when the pumping was performed, and therefore there is no direct data to investigate its performance at that time (summer of 2018). However, Figures 15 (right) and 16 (right) can be used to assess the overall detector performance immediately before the detector failure and after its recovery, which occurred several months after the pumping. The gap in the figures refers to the period of the detector down time and as can be seen from the Pu ratios, the performance is consistent before and after the recovery indicating that pumping performed during that timeframe had not adverse effect.

8.2. Neutron system troubleshooting

Noise in IPCA2 neutron signal was observed on several channels during October 2018 control measurements. Troubleshooting was performed to evaluate grounding of the IPCA2 external body and its tie-rods. The noise was mitigated by more secure grounding of the tie-rods inside IPCA2. Possible cause of this sudden noise was attributed to cell-phone repeaters, which were installed in the building housing IPCA2 shortly prior to start of the measurements. Neutron count rates are continuously monitored in the background mode as well as during monthly measurements to confirm absence of noise issues.

9. Updates to measurement procedure

This section discusses minor updates to measurement procedures proposed for the future control measurements, in order to improve performance and uncertainty.

We propose to unify measurement times per cycle for all the IPCA2 neutron measurements. Currently, the stability measurements (AmLi and Cm) are performed using 100s cycles for 3600 s total measurement time (i.e. 36 x 100s) and Pu efficiency is performed using 30 s cycles for 1800 s (i.e. 60 x 30s). For uncertainty calculation using sample based error it is most suitable to perform measurements with high number of cycles. Therefore, we recommend to use 30 s cycles also for the stability measurements with AmLi and Cm. The total measurement times will remain unchanged for stability measurements, but will be performed with 30 s cycles over 3600 s (i.e. 120 x 30 s, instead of original 36 x 100s).

We recommend to increase the total measurement time for the efficiency measurements to 7200 s from 1800 s. IPCA2 is designed to provide Pu-mass assay with ~1% uncertainty, however the efficiency monitoring measurements exhibit generous 3σ control bounds, corresponding to ~3%. The count rate measured from FZC158 Pu standard is fairly low (~60 counts per second), which explains the sizeable error bars in the individual efficiency measurements (Figures 1-4) in 1800 s measurement time and the noticeable spread of the individual measurements as a function of time. To improve the fidelity of the efficiency measurements, we recommend to increase the measurement time by a factor of 4 (to 7200 s), in order to reduce the uncertainty of individual measurements by a factor of 2 and reduce the spread of the 3σ control bounds.

10. Summary

Table 1 provides and overview of all the control measurements performed over the reporting period (October 2018 – March 2019). Note that October includes higher number of measurements due to troubleshooting activities that were performed that month.

Table 1: The number of measurements taken monthly organized by type.

Month	Pu Eff	AmLi	Cm	12698B (Top)	41993A (Middle)	4200A (Bottom)	Load Cell
October 2018	8	10	7	7	5	0	7
November 2018	3	3	3	3	3	0	3
January 2019	3	3	3	3	3	3	3
February 2019	2	2	2	2	2	1	2
March 2018	1	1	1	1	1	1	1
Total	17	19	16	16	14	7	16

Results of individual monthly control measurements were provided to JAEA in monthly reports [2-5]. This report provides a summary of annual performance of IPCA2 during the reporting period of October 2018 through March 2019.

It is found that plutonium efficiency showed stability and stayed within 2σ of the overall average value of 7.35 % established from 2013-2017 data in reference [1]. No dependence on environmental conditions (temperature, humidity) was observed. The average efficiency of these measurements (performed between October 2018 and March 2019) corresponds to 7.29 ± 0.04, which is slightly below the previously extracted 7.35%, but within 3σ. Updated control bounds were established based on this dataset (see Appendix A).

The AmLi stability measurements over the reporting period showed good performance, typically within 3σ of the overall average value established in reference [1]. No dependence on environmental conditions (temperature, humidity) was observed. The average count rate (decay corrected count with respect to 01/12/2017) for measurements performed between October 2018 and March 2019 corresponds to 24484 ± 33, which is slightly below the previously extracted value of 24541, but within 3σ. Updated control bounds were established based on all JFY18 data and are reported in Appendix A.

Curium source measurements were performed to evaluate its feasibility as a potential replacement for the AmLi source to mitigate issues observed in AmLi measurements [1] due to redistribution of source material and positioning. The average count rate (decay corrected with respect to the first measurement on 10/15/2018) for measurements performed between October 2018 and March 2019 corresponds to 987.3 ± 2.0. No dependence on environmental conditions (temperature, humidity) was observed. Results were used to establish new control bounds as documented in Appendix A. Based on the trends observed so far, Curium appears to be a viable alternative to AmLi sources. Both sources will continue to be used during JFY19 control measurements.

HPGe system monitoring revealed consistent performance of the top detector (12698B) within the 3σ of expected performance, with the exception of several November 2018 through January 2019 $^{241}Pu/^{239}Pu$ ratios and December 19 measurement, likely caused by temporary reduction and later complete failure of cooling performance. The cooling, however, appears to have been restored as the January-March 2019 data exhibit trends within 3σ control bounds. The middle detector (41993A) exhibits performance within 3σ control bounds over the entire reporting period. The bottom detector (4200A) system was not functional until January 2019, when the original X-Cooler was replaced using a LANL spare. The detector then exhibited target performance during the subsequent months. The HPGe detector results from this reporting period were used to extract updated control bounds reported in Appendix A. The control bounds for the bottom detector remain the same due to limited number of measurements performed.

In summary, the neutron system performance exhibits expected trends and measurements will continue on monthly basis in JFY19. The HPGe system reveals multiple issues mostly related to failure of cooling modules, but also data acquisition electronics, likely due to limited lifetime of the system components. Since it is anticipated that the entire HPGe system will be replaced by new instrumentation before its installation at J-MOX, the HPGe measurements will be reduced to twice-a-year for JFY19 control period.

11. References

[1] M.T. Andrews, M.T. Swinhoe, J. Archuleta, D. Henzlova, A. Favalli, J.B. Marlow, "IPCA 2 Data Analysis and Updated Control Charts", Los Alamos National Laboratory Technical Report, LA-CP-20366 (2017).

[2] M.T. Andrews, J. Archuleta, A. Favalli, D. Henzlova, C.D. Rael, J.B. Marlow, M.T. Swinhoe, October 2018 IPCA 2 Report, Los Alamos National Laboratory Technical Report, LA-CP-18-20791 (November 2018)

[3] D. Henzlova, J. Archuleta, M.T. Andrews, A. Favalli, J.B. Marlow, C.D. Rael, M.T. Swinhoe, November 2018 IPCA 2 Report, Los Alamos National Laboratory Technical Report, LA-CP-18-20842 (December 2018)

[4] D. Henzlova, J. Archuleta, A. Favalli, M.T. Andrews, J.B. Marlow, C.D. Rael, M.T. Swinhoe, December 2018 IPCA 2 Report, Los Alamos National Laboratory Technical Report, LA-CP-19-20016 (January 2019)

[5] D. Henzlova, J. Archuleta, M.T. Andrews, A. Favalli, J.B. Marlow, C.D. Rael, M.T. Swinhoe, January 2019 IPCA 2 Report, Los Alamos National Laboratory Technical Report, LA-CP-19-20070 (January 2019)

12. Appendix A

This Appendix provides an overview of updated control bounds calculated from JFY18 data that will be used during JFY19 control measurements.

12.1. Updated AmLi control bounds from JFY18 data

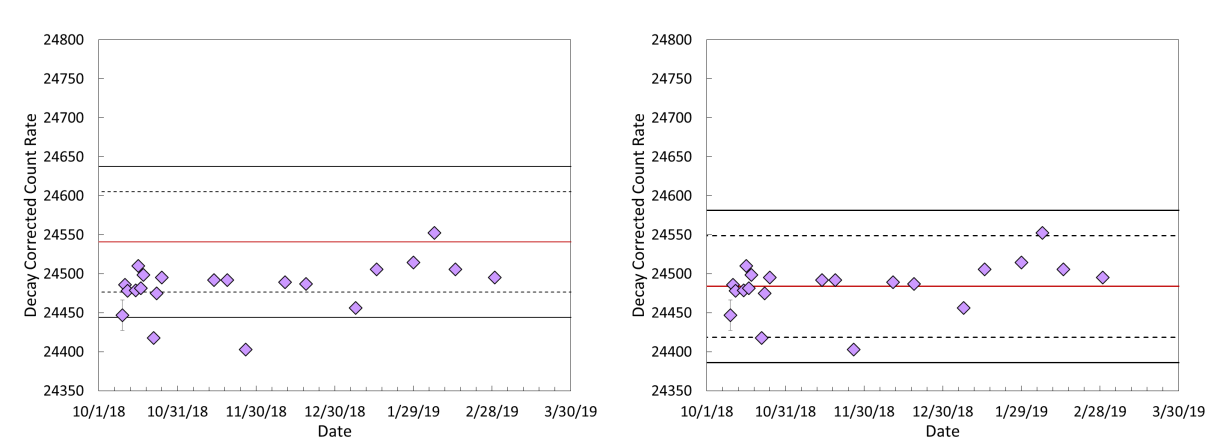

Figure 21: AmLi stability control bounds; original [1] (left); updated based on JFY18 data (right).

12.2. Updated Cm control bounds from JFY18 data

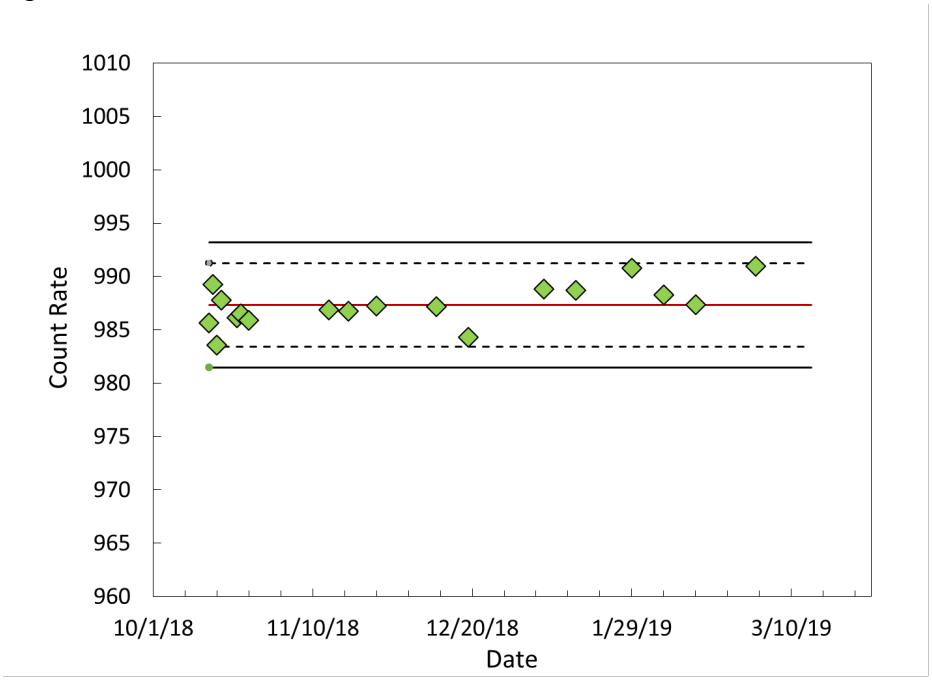

Figure 22: Cm stability control bounds established based on JFY18 data.

12.3. Updated efficiency control bounds from JFY18 data

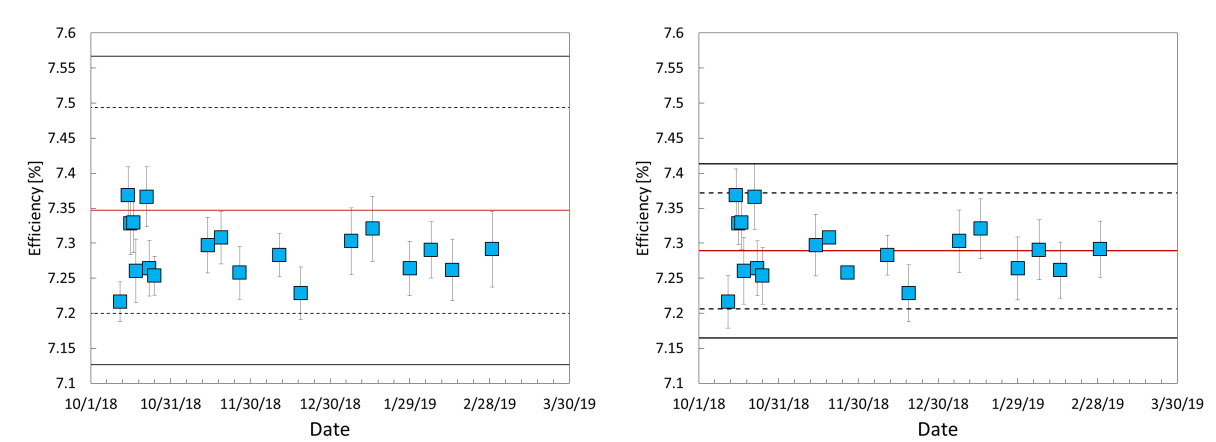

Figure 23: FZC158 efficiency control bounds; original [1] (left); updated based on JFY18 data (right).

12.4. Updated top HPGe detector control bounds

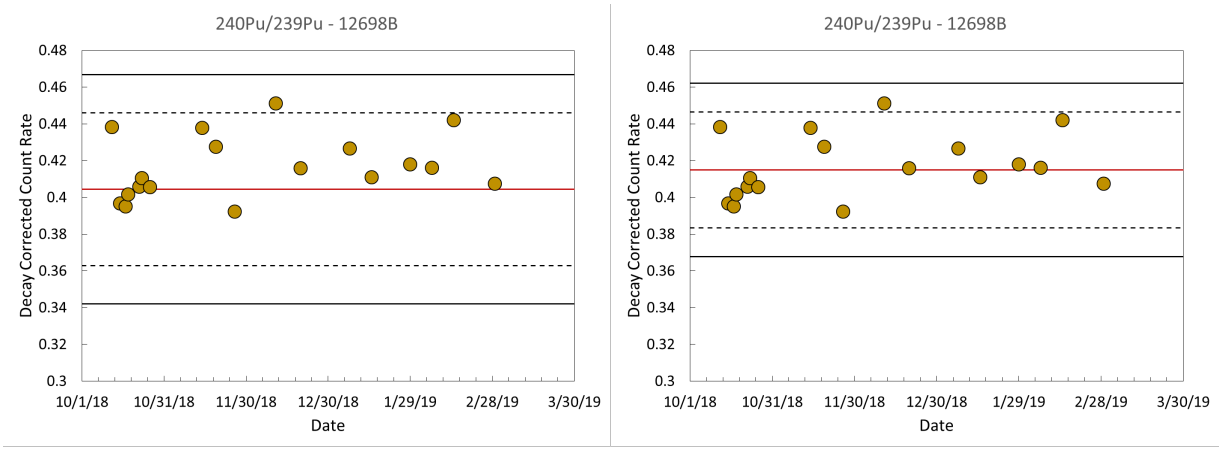

Figure 24: Top HPGe detector control bounds for $^{240}Pu/^{239}Pu$; original [1] (left); updated based on JFY18 data with December 19 measurement excluded (right).

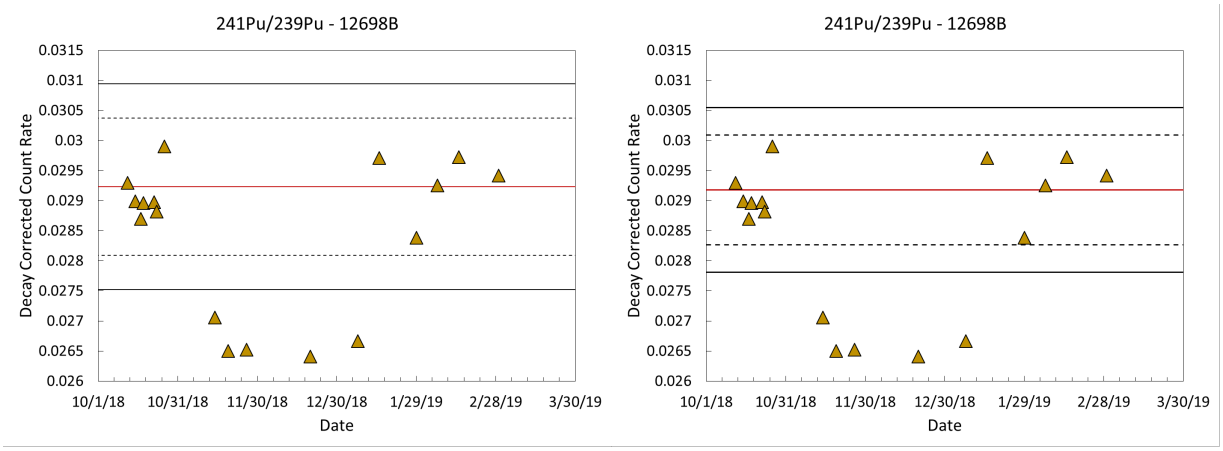

Figure 25: Top HPGe detector control bounds for $^{241}Pu/^{239}Pu$; original [1] (left); updated based on JFY18 data with measurements outside the original 3σ excluded (right).

12.5. Updated middle HPGe detector control bounds

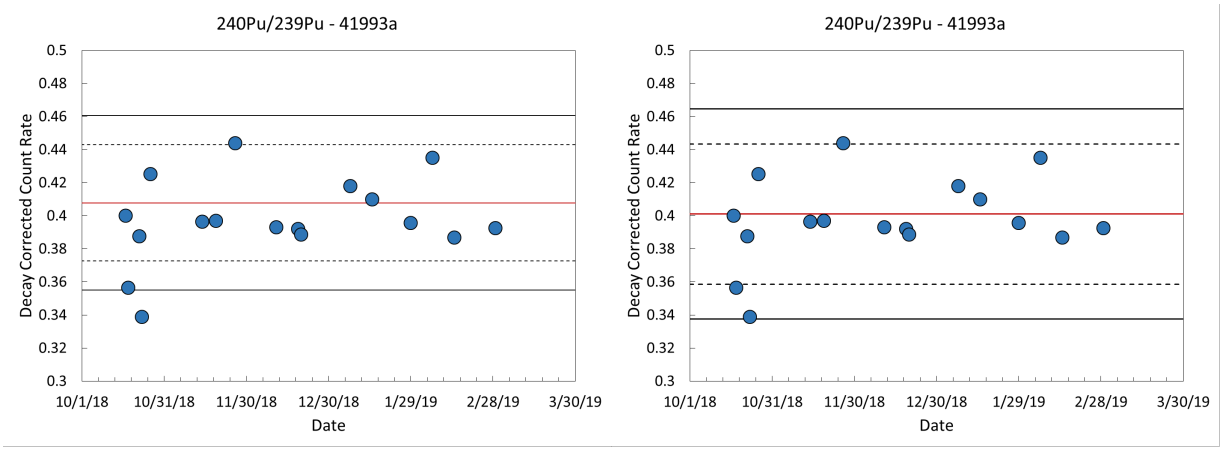

Figure 26: Middle HPGe detector control bounds for $^{240}Pu/^{239}Pu$; original [1] (left); updated based on JFY18 data with measurement outside the original 3σ excluded (right).

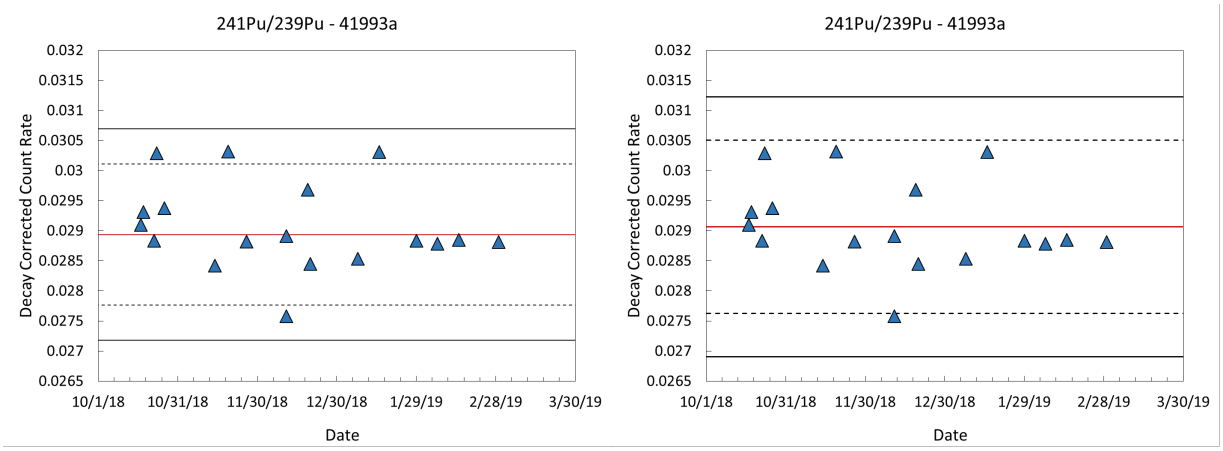

Figure 27: Middle HPGe detector control bounds for $^{241}Pu/^{239}Pu$; original [1] (left); updated based on JFY18 data (right);

12.6. Bottom HPGe detector control bounds

Updated control bounds for the bottom detector were not established due to the limited number of measurements performed with this detector during the reporting period. The original control bounds, shown in Figures 29 and 30 will be used in JFY19.

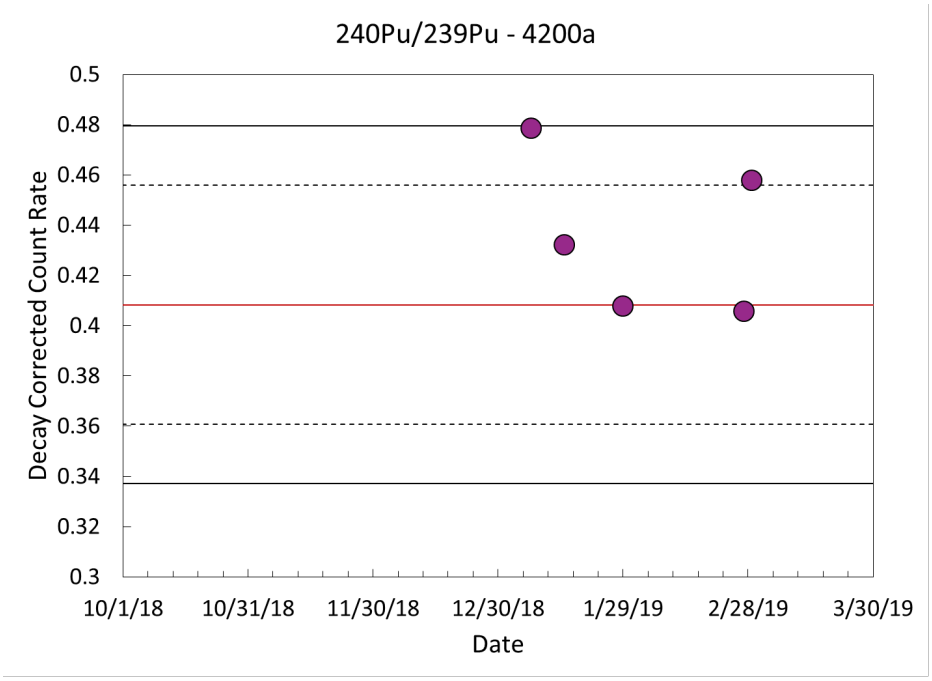

Figure 28: Original [1] bottom HPGe detector control bounds for $^{240}Pu/^{239}Pu$ shown with JFY18 data.

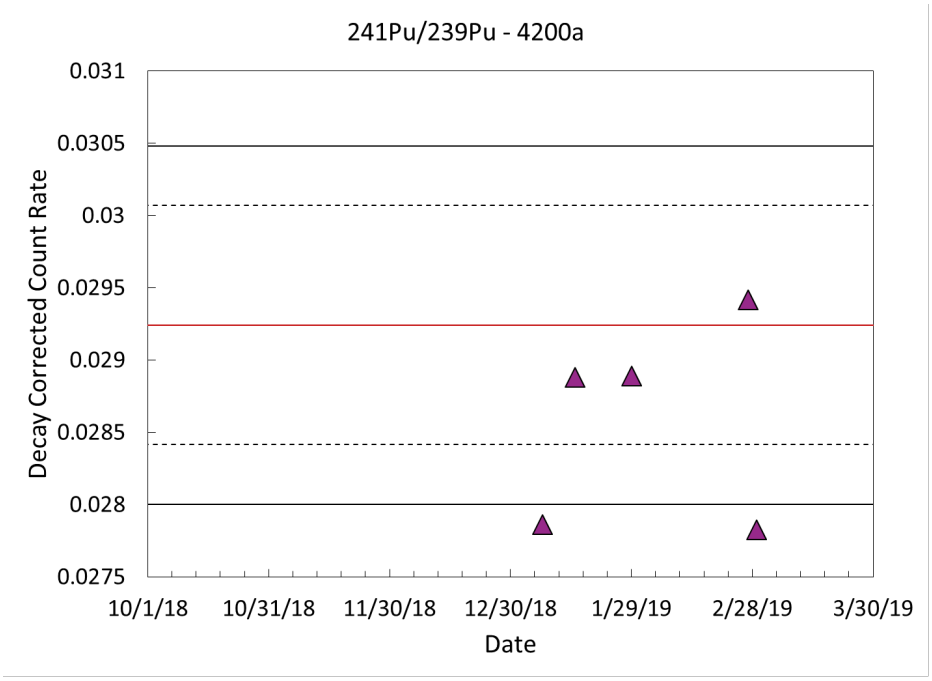

Figure 29: Original [1] bottom HPGe detector control bounds for $^{241}Pu/^{239}Pu$ shown with JFY18 data.